# Comparison of CLT buckling strength criteria with experimental results

Alma Narcy, Gilles Forêt, Duc Toan Pham, Arthur Lebée

# Comparison of CLT buckling strength criteria with experimental results

A. NARCY, D. T. PHAM- Centre Scientifique et Technique du Bâtiment (CSTB)

G. FORÊT, A. LEBEE- Laboratoire Navier (Ecole des Ponts ParisTech,

Université Gustave Eiffel, CNRS UMR 8205)

Keywords: CLT Panels, Buckling Strength, Eccentricities, Shear, Imperfections, Experiments

## 1 Introduction

The growth of wood high-rise building construction is being facilitated by new timber structural elements such as Cross Laminated Timber (CLT) panels.

Their use as load-bearing walls questions their buckling strength and the corresponding design method as well as the mechanical characteristics that should be taken into account or not, such as their highly anisotropic and heterogeneous behavior. For instance, *Pina* et al. (2019) studied the influence of the number of layers on the buckling capacity of centered loaded CLT panels, *Karacabeyli* & *Gagnon* (2020) indicated that only longitudinal layers should be taken into account when studying buckling of these elements. *Thiel* & *Krenn* (2016) studied with a FEM model the influence of CLT layup, shear flexibility due to rolling shear modulus, and the panel's width on the panel's buckling capacity, they concluded that shear flexibility could be neglected for buckling studies.

The derivation of a unified yet simple design approach for CLT structural walls is still debated. *Theiler* et al. (2012) compared two buckling design methods for solid timber: Equivalent Length Method (ELM) used in Eurocode 5 EN 1995 1-1 (2005), and the second-order structural analysis that takes into account geometric non-linearity. *Kudo* et al. (2018) compared CLT buckling experimental strength of CLT panels to predicted values obtained with Japanese Building Code and concluded that the latter gives a good evaluation. *Perret* et al. (2020) proposed an analytical buckling strength criterion for CLT panels with imperfection, assuming shear failure. *Huang* et al. (2022) and *Shen* et al. (2022) compared buckling design formula from Canadian code CSA O86 and Chinese standard GB/T 51226, with experimental buckling strength of CLT panels as a function

of load eccentricity. They showed that both formulas are conservative, and proposed a model fitting more closely to experimental values.

Design methods should also be experimentally validated. However, test results are mostly compared to material scale strength and stiffness moduli (*Wang* et al. (2016); *Huang* et al. (2022); *Shen* et al. (2022)) whereas strength criteria are directly based on structural moduli. This requires theoretical models to determine structural axial, bending and shear stiffness and strength. Hence, approximations are inevitably made as soon as panel properties are estimated from material parameters (*Christovasilis* et al. (2016)) and the accuracy of the comparison between tests and criteria remains debatable.

The present study compares buckling tests of CLT panels with and without load eccentricities to several buckling criteria from the literature. A total of seventeen 5-ply CLT panels were tested in buckling. The structural properties of panels were determined: bending and shear stiffness, as well as the compression, bending and rolling shear strength of the tested panels that have been directly measured. The bending stiffness and equivalent imperfection, taking into account defect of rectitude, load position uncertainty and neutral axis offset, have been measured for each tested panel by means of a linear regression presented in this paper. As these two parameters have a strong influence on the predicted strength of each panel, their determination enables a more relevant comparison of criteria. Moreover, the determination of the equivalent imperfection indicates the sensitivity of this parameter and its influence when studying experimental buckling behavior.

Finally, buckling criteria are compared to experimental results. It shows that the consideration of shear in Eurocode 5 lowers the deviation of predicted failure force to experimental results and that the Non-Linear Criterion features the lower relative deviation.

# 2 Critical buckling loads, elastic strength criteria and design methods

Buckling strength criteria are classically derived in three steps. First, a beam model is chosen and a critical load is derived from stability considerations. Second, imperfections are introduced such as rectitude defect of elements or load eccentricity in order to predict correctly the weakly non-linear amplification of the deformation caused by the primary load $P$. Finally, a local strength criterion is chosen in order to predict the failure of the non-linear beam model.

Regarding timber column, Euler's beam model is usually retained. Euler's stability buckling criterion writes as:

$$p < \frac{1}{\lambda_{\text{Euler}}^2} \quad \text{where} \quad p = \frac{P}{P_u} \quad \text{and} \quad \lambda_{\text{Euler}} = \sqrt{P_u \left( \frac{L^2}{\pi^2 \, EI} \right)} \tag{1}$$

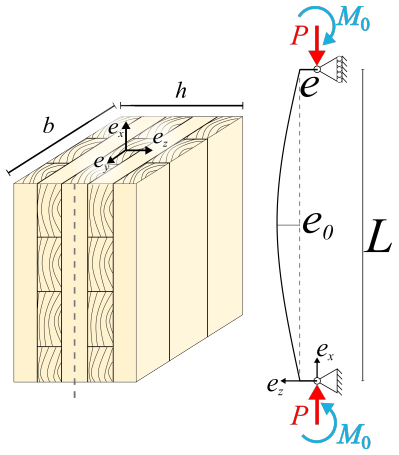


*Figure 1. CLT panel and double-hinged column*

where $\lambda_{\text{Euler}}$ is the relative slenderness of the column, accounting for its stiffness and strength. $L$ stands for the buckling length, $EI$ the bending stiffness and $P_u$ the ultimate compressive load $P_u = f_c S_{eq}$, with $f_c$ is the compressive strength, and $S_{eq}$ is the equivalent sectional area taking into account only longitudinal layers. This model ignores shear, despite the fact that CLT panels are known to be significantly shear-compliant. A relative slenderness accounting for shear stiffness $GS$ can thus be introduced, corresponding to Timoshenko's beam model (see *Perret* et al. (2020), among others):

$$\lambda_{\text{Timo.}} = \sqrt{P_u \left( \frac{L^2}{\pi^2 EI} + \frac{1}{GS} \right)} \tag{2}$$

Thereafter, imperfections are modeled either as a small sinusoidal rectitude defect $e_0$ or a uniform eccentricity $e$ (Wang et al., 2016; Huang et al., 2022; Shen et al., 2022) and sometimes as an additional uniform and constant bending moment $M_0$ as in Figure 1.

Finally, a failure criterion related to an excess of compression and bending at mid-span of the panel is chosen:

$$\frac{P}{P_u} + \frac{M}{M_u} < 1 \tag{3}$$

where $M$ is the equivalent moment considering all induced moments ($Pe_0$ due to initial rectitude defect, $Pe$ due to load eccentricity and $Pf$ due to the beam deflection), and additional moment $M_0$. $M_u$ is the ultimate bending moment.

From the constitutive law and beam kinematics, we can write $f'' - \frac{M}{EI} = 0$, where $f$ is the panel's deflection. Taking into account double-hinged boundary conditions, the expression of $f$ along the column can be identified, and the maximal bending moment $M_{\text{max}}$ that is reached at the panel's mid-height:

$$M_{\text{max}} = (M_0 + Pe) \frac{1}{\cos\left(l\sqrt{\frac{P}{EI}}\right)} - Pe_0 \frac{1}{1 - \frac{P}{P_{cr}}} \tag{4}$$

where $P_{cr}$ is the critical buckling load, defined as:

$$\frac{1}{P_{cr}} = \frac{1}{P_E} + \frac{1}{GS} \quad \text{where} \quad P_E = EI\frac{\pi^2}{L^2} \tag{5}$$

Considering all moments, a non-linear relation appears, due to the moment amplification that is not the same depending on the moment distribution. It is the case for the amplification of an initial constant moment $M_0$, and the one of the moment due to a load eccentricity $e$. Consequently, the following approximation is classically introduced:

$$\frac{1}{\cos\left(l\sqrt{\frac{P}{EI}}\right)} \approx \frac{1+\delta\frac{P}{P_{cr}}}{1-\frac{P}{P_{cr}}} \tag{6}$$

where $\delta = \frac{\pi^2}{8} - 1 = 0.234$ is the approximation factor sometimes called Dutheil (*Maitre* (2013)) or Dischinger coefficient (*Lindner* et al. (2016), *van Delft* (2020)). Thanks to this approximation, the elastic failure criterion may write as a second-order polynomial criterion in $p$, herein called Non-Linear Criterion (NLC):

$$p^2\left(\frac{e\delta}{e_n} - 1\right) + p\left(1 + \frac{1}{\lambda^2} + \frac{1}{e_n}\left(\frac{e_0+e}{\lambda^2} + \frac{M_0\delta}{P_u}\right)\right) - \frac{1}{\lambda^2} + \frac{M_0}{P_u e_n \lambda^2} \leq 0 \tag{7}$$

where $e_n = \frac{M_u}{P_u}$ . In this model, $\lambda = \lambda_{\text{Timo.}}$.

In the present paper, this criterion is compared to the current version of the Eurocode 5 (EN 1995 1-1, 2005) that assesses the stability of members using a bending-compression criterion:

$$\frac{p}{k_c} + m < 1 \tag{8}$$

where $m$ is the normalized first-order moment considering the moments the column is subjected to ($Pe$ and $M_0$), without amplifying them, and $k_c$ stands for the buckling factor, which takes into account the amplification of the moment due to an initial rectitude defect. It writes as:

$$k_c = \frac{1}{k_y + \sqrt{k_y^2 - \lambda^2}} \quad \text{with} \quad k_y = \frac{1}{2}\left(1 + \beta_0\lambda + \lambda^2\right) \tag{9}$$

It assumes an arbitrary imperfection $\beta_0 = 0.1$ related to rectitude defect (*Blaß* & *Ehlbeck* (1987)). Thereafter, EC5 stands for Eurocode 5 ignoring shear deformations by taking $\lambda = \lambda_{\text{Euler}}$, and $\text{EC5}_{\text{G}}$ takes shear deformations into account by taking $\lambda = \lambda_{\text{Timo.}}$.

# 3 Panel characterization and buckling tests

The studied CLT panels are 5-ply panels, 100 mm thick and 500 mm wide, made of C24 timber. They come from Pfeifer. Their mean density is 484 kg/m$^3$ with a coefficient of variation (CV) of 4%. All panels originate from the same batch and have been kept in a climatic chamber at 21°C (CV 1%), and 63% relative humidity (CV 0.3%) for at least two months. A characterization campaign was conducted on small samples obtained from trimmed CLT. Compression and bending tests were conducted. Then, buckling tests were conducted on CLT panels with three heights and three eccentricities.

## 3.1 Panel characterization

In order to compare critical buckling loads, elastic strength criteria and design methods with experimental results, the equivalent slenderness $\lambda$ of tested panels needs to be determined, which is based on $GS$ and $EI$. $GS$ is determined using bending tests, and $EI$ is determined either using bending tests or directly during the buckling test. Furthermore, the ultimate compressive force $P_u$ and the ultimate moment $M_u$ are determined using compression tests and bending tests.

### *3.1.1 Compression tests*

33 CLT samples (height = 150 mm, sectional area = 100x70mm$^2$) have been tested in compression until failure. Failure is considered when the maximal force is reached. We measure a mean maximal force which is equivalent, for large panels (100 mm thick, 500 mm wide), to $P_u = 1.26$ GN (CV 8%). It gives a mean compression strength of longitudinal layers $f_{c,mean} = 42$ MPa (CV 8%). The characteristic compressive strength indicated by Pfeifer GmbH, 2021 is: $f_{c,k} = 21$ MPa.

### *3.1.2 Bending tests*

9 CLT panels have been tested in bending using four-point bending tests. Two different dimensions were tested. 6 small panels (1450x100x250mm$^3$) were tested with a span $l = 1150$ mm and a distance between the two application points of force $P$ such as $l_0 = 250$ mm. This distance was chosen to ensure a sufficient shear contribution to the total deflection. By means of LVDTs, rotations at supports $\Delta\varphi$ (assuming small rotation) and total deflection $f$ were measured. $EI$ and $GS$ were then determined according to *Perret* et al., 2018:

$$EI = \frac{P(l^2 - l_0^2)}{8\Delta\varphi} \quad , \quad \frac{1}{GS} = \frac{4f}{P(l - l_0)} - \frac{1}{8EI}\left(l^2 - \frac{1}{3}(l - l_0)^2\right) \tag{10}$$

For each tested sample, $EI$ is obtained and then used to determine $GS$. We measured a mean bending stiffness which is equivalent, for large panels (100 mm thick, 500 mm wide), to $EI = 428$ GN.mm$^2$ (CV 9%) and a mean shear stiffness $GS = 23.8$ $MN$


*Figure 2. Typical buckling test*

(CV 3%). All 6 panels failed in rolling shear, which gave a mean rolling shear strength of $f_{v,mean}$ = 1.4 MPa (CV 6%). The characteristic rolling shear strength indicated by Pfeifer GmbH, 2021 is: $f_{v,k}$ = 1.3 MPa.

Three other large panels (2900x100x500mm$^3$) were tested, until bending failure, with $l$ = 2300 mm and $l_0$ = 700 mm. The mean ultimate moment measured was $M_u$ = 28.5 MN.mm (CV 13%), which gives a mean bending strength $f_{m,mean}$ = 40.9 MPa (CV 13%). The characteristic bending strength indicated by Pfeifer GmbH, 2021 is: $f_{m,k}$ = 24 MPa.

## 3.2 Buckling tests

### *3.2.1 Experimental setup*

17 CLT panels of 3 different lengths (1450, 1930 and 2900 mm), with a width of 500 mm, have been tested in compression. The boundary conditions are such that both ends of the panel are articulated: no deflection but free rotation, see Figure 2. The bottom end of the panel is kept fixed in vertical and out-of-plane translations, while its top end is free to translate vertically. The distance between the ends of the panels and the rotation axis is 12.8 cm, which gives buckling lengths $L$ of 1706, 2186 and 3156 mm. Three loading eccentricities were tested: 0, 10 and 20 mm. During the tests, the applied load and the resulting displacement evolution are continuously recorded by a data acquisition system. A typical CLT panel and the experimental set-up are shown in Figure 2. The measurement of the displacement is performed by means of LVDTs. Strains at mid-height of the panel are measured with strain gauges on each face.

### *3.2.2 Results*

All panels failed in compression on one side of the panel (see Figure 2), a secondary failure in tension is observed on the opposite side, sometimes followed by rolling shear

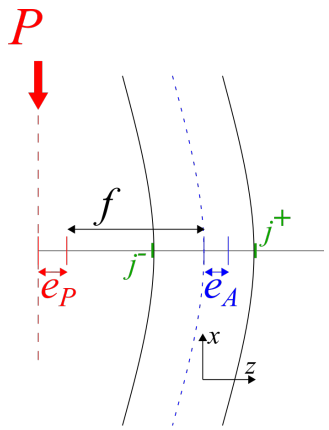


*Figure 3. Panel's imperfection, load $P$, load centering uncertainty $e_P$, neutral axis uncertainty $e_A$, deflection $f$, deformation $j^+$ and $j^-$*

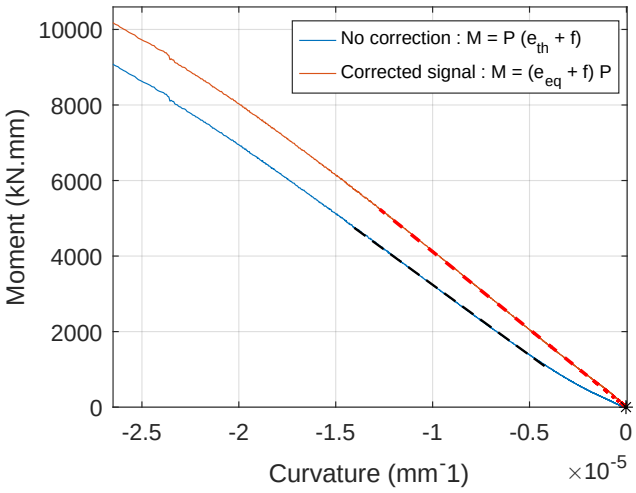


*Figure 4. Moment before and after signal correction (Panel 24)*

failure in transverse lamellae. The maximal compressive forces are indicated in Table 1 for each panel. We also estimate $ES$, $EI$ and $e_{eq.}$ which includes all imperfections (load eccentricity $e$, load location uncertainty $e_P$, and deviation of the neutral axis from the symmetrical axis of the panel $e_A$), as presented in Figure 3. $ES$ is obtained from the vertical displacement $\Delta L$ measured with LVDT, from the classical relation:

$$F = ES\,\bar{\varepsilon} = ES\,\frac{\Delta L}{L} \tag{11}$$

The elasticity modulus of layers along the longitudinal direction $E_L$ is determined from $ES$ assuming equivalent section $S_{eq}$. The mean value for all panels is $E_L = 14$ GPa (CV 10%). The corresponding value indicated by Pfeifer GmbH, 2021 is: $E_{L,mean} = 11$ GPa.

Due to imperfections and load eccentricity, the actual moment of the beam at mid-span writes as:

$$M = (e_{eq.} + f)\,P \tag{12}$$

where $e_{eq.}$ is the equivalent imperfection that includes $e$, $e_0$, $e_P$ and $e_A$. From the constitutive law, we have:

$$M = EI\kappa \tag{13}$$

where $\kappa$ is the beam curvature that can be measured with strain gauges ($j^+ - j^-$) as $\kappa = \frac{j^+ - j^-}{h}$.

We can thus write:

$$(e_{eq.} + f)\,P = EI\,\frac{j^+ - j^-}{h} + a \tag{14}$$

From this equation, $e_{eq.}$ and $EI$ are obtained using the Least Square method applied to

*Table 1. Buckling tested panels, mechanical and geometrical characteristics, and maximal force (experimental and theoretical).*

| Panel | Density (kg/m$^3$) | Height (mm) | $e_{th.}$ (mm) | $e_{eq.}$ (mm) | Diff. (mm) $e_{eq.}$, $e_{th.}$ | $EI$ (kN.mm$^2$) | $ES$ (kN) | $\lambda_G$ | $P_{max}^{expe.}$ (kN) | $P_{max}^{EC5}$ (kN) | $P_{max}^{NLC}$ (kN) |
|---|---|---|---|---|---|---|---|---|---|---|---|
| 1 | 476 | 2900 | 0 | 0,4 | 0,4 | 4,17E+08 | 3,50E+05 | 2,20 | 379 | 378 | 401 |
| 2 | 490 | 2900 | 0 | 3,5 | 3,5 | 4,54E+08 | 4,50E+05 | 2,11 | 393 | 391 | 398 |
| 13 | 524 | 2900 | 20 | 16,1 | -3,9 | 4,93E+08 | 4,89E+05 | 2,02 | 291 | 351 | 322 |
| 14 | 503 | 2900 | 20 | 25,5 | 5,5 | 5,40E+08 | 4,93E+05 | 1,93 | 335 | 331 | 301 |
| 161 | 481 | 1450 | 0 | 2,2 | 2,2 | 3,26E+08 | 4,54E+05 | 1,35 | 892 | 812 | 762 |
| 162 | 484 | 1450 | 20 | 14,1 | -5,9 | 5,16E+08 | 4,04E+05 | 1,07 | 480 | 690 | 628 |
| 171 | 488 | 1450 | 0 | 3,5 | 3,5 | 5,36E+08 | 4,73E+05 | 1,05 | 880 | 952 | 907 |
| 172 | 497 | 1450 | 20 | 11,7 | -8,3 | 5,11E+08 | 4,29E+05 | 1,07 | 480 | 732 | 653 |
| 21 | 470 | 1450 | 0 | 4,1 | 4,1 | 6,20E+08 | 4,13E+05 | 0,98 | 998 | 960 | 961 |
| 23 | 477 | 1450 | 20 | 19,3 | -0,7 | 4,50E+08 | 3,98E+05 | 1,15 | 511 | 593 | 510 |
| 24 | 491 | 1445 | 0 | 1,4 | 1,4 | 4,12E+08 | 3,64E+05 | 1,20 | 813 | 943 | 982 |
| 25 | 423 | 1455 | 10 | 10,8 | 0,8 | 3,98E+08 | 3,96E+05 | 1,22 | 688 | 701 | 589 |
| 26 | 482 | 1930 | 10 | 7,5 | -2,5 | 3,78E+08 | 4,68E+05 | 1,60 | 504 | 565 | 491 |
| 27 | 489 | 1930 | 20 | 26,0 | 6,0 | 3,94E+08 | 3,88E+05 | 1,57 | 454 | 416 | 349 |
| 28 | 485 | 1930 | 20 | 21,9 | 1,9 | 5,39E+08 | 3,95E+05 | 1,34 | 506 | 512 | 476 |
| 29 | 485 | 1930 | 10 | 11,9 | 1,9 | 4,37E+08 | 4,25E+05 | 1,49 | 597 | 566 | 494 |
| 31 | 485 | 1930 | 0 | 0,7 | 0,7 | 3,56E+08 | 4,09E+05 | 1,65 | 668 | 626 | 670 |
| **Moy.** | **484** | | | | **0,6** | **4,58E+08** | **4,25E+05** | | | | |
| **Std. Dev.** | **20** | | | | **3,9** | - | - | | | | |
| CV (%) | 4 | | | | - | 17 | 10 | | | | |

the signals of each panel, with $a$ the linear regression constant that remains negligible as signal offsets are removed at the beginning of the tests. Using $e_{eq.}$ instead of $e_{th.}$ in the derivation of the bending moment has a significant influence at low load levels, as shown in Figure 4.

Finally, all mechanical characteristics are gathered (see Table 1) to calculate the predicted strength for each panel using the different models.

Let us readily point out that the mean difference between theoretical eccentricity and the estimated equivalent imperfection is 0.6 mm (see Table 1), with a standard deviation of 3.9 mm. It gives an indication of the experimental precision, and the significance of precisely measuring the equivalent imperfection, especially for this order of magnitude of theoretical imperfection (0, 10 and 20 mm).

# 4 Comparison of experimental results and estimated maximal force

First, the experimental results of buckling tests are presented with a normal force-bending moment interaction diagram. Then, the results are presented for each panel, as well as the strength predicted by the models. Finally, the deviation of each model to experimental results, depending on the parameters used in models are presented.

## 4.1 Interaction diagram

The normal force-bending moment interaction diagram is plotted for CLT panels tested in buckling. For each panel, $P_{max}$ and its corresponding moment are normalized with $P_u$

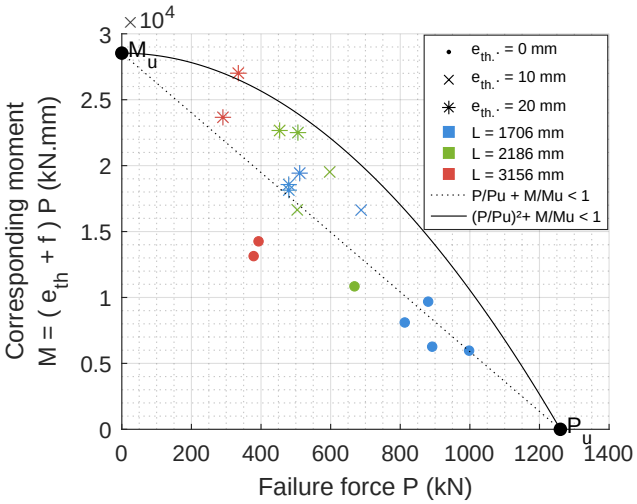


*Figure 5. Interaction diagram without correction, $M = (e_{th.} + f)P$*

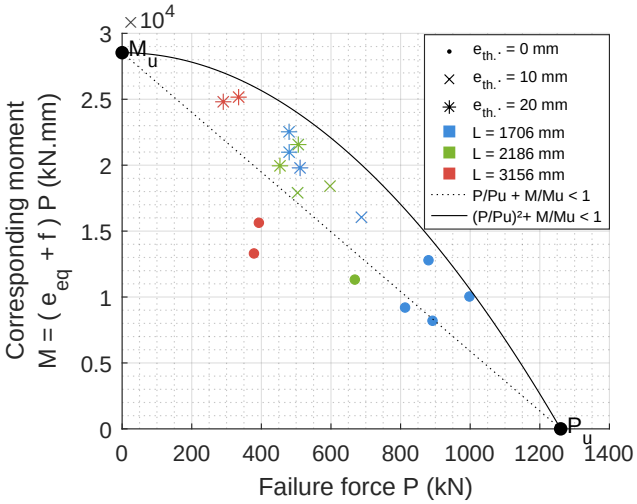


*Figure 6. Interaction diagram with corrected signal, $M = (e_{eq.} + f)P$*

and $M_u$, and plotted. Also, the interaction formula for columns subjected to combined axial and bending force as presented in EN 1995 1-1 (2005) (Section 6.2.4) is plotted for two cases. The first case assumes a moment measured with deflection and $e_{\text{th.}}$, and the second case uses $e_{\text{eq.}}$ instead. Deriving the failure bending moment from $e_{\text{th.}}$ tends to underestimate it, especially for short panels. We also observe that the influence of imperfection is larger for shorter panels: short panels with small load eccentricity feature significantly larger failure force than similar panels with large load eccentricity (20 mm). Nevertheless, it is less the case for more slender panels.

## 4.2 Buckling experimental results and predicted strengths with models

The following approach is adopted to compare the critical buckling length, elastic strength criterion, and design methods for all the tested panels. The predicted compressive strength $p = P/P_u$ is calculated according to each model, that are Eurocode 5 (Equation 8), with either $\lambda_{\text{Euler}}$ (*EC*5) or $\lambda_{\text{Timo.}}$ ($EC5_G$), and the Non-Linear Criterion (***NLC***, Equation 7) with $\lambda_{\text{Timo.}}$.

For each criterion, two cases are investigated. The first case uses average parameters (mean *EI* and *GS* from bending tests) to predict panel strength, as well as the theoretical load eccentricity $e_{\text{th.}}$ (0, 10 or 20 mm), and an arbitrary initial rectitude defect $e_0 = 1$ mm chosen according to measured values on tested panels. The second option uses parameters specific to each panel: *EI* and $e_{\text{eq.}}$, measured during buckling tests and indicated in Table 1. A mean value of *GS* obtained during bending is used, as it may not be determined during buckling tests. Also, the initial rectitude defect is set to $e_0 = 0$ mm as $e_{\text{eq.}}$ already takes it into account. For both cases, the mean value of $f_c$ obtained with compression tests is used.

Figure 7 presents, for each tested panel, the three normalized predicted forces obtained with average parameters from bending tests. Figure 9 presents the same comparison, using measured parameters *EI* and $e_{\text{eq.}}$ for each panel, and the experimental force. We

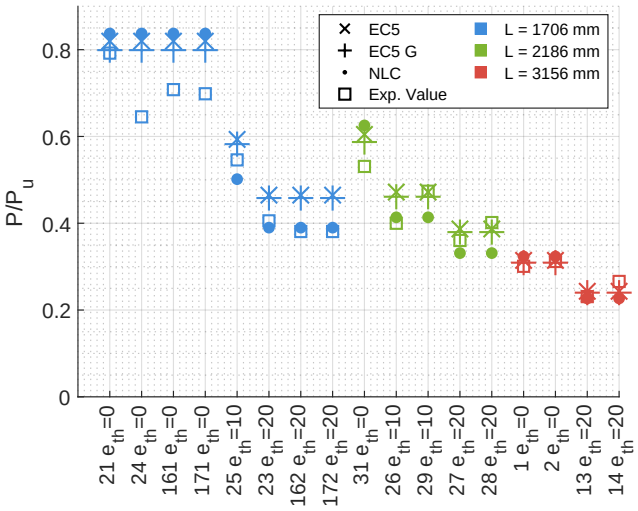


*Figure 7. Comparison between predicted strength with models using average **EI** and $e_{th.}$ for each panel, and experimental values.*

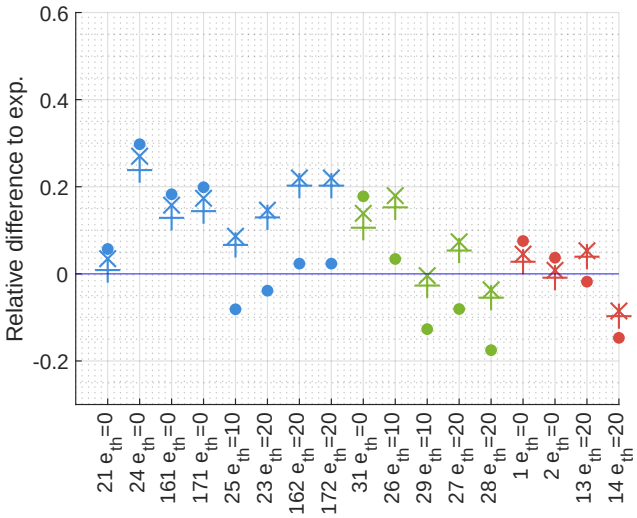


*Figure 8. Relative difference from predicted forces to experimental results, using average **EI** and $e_{th.}$.*

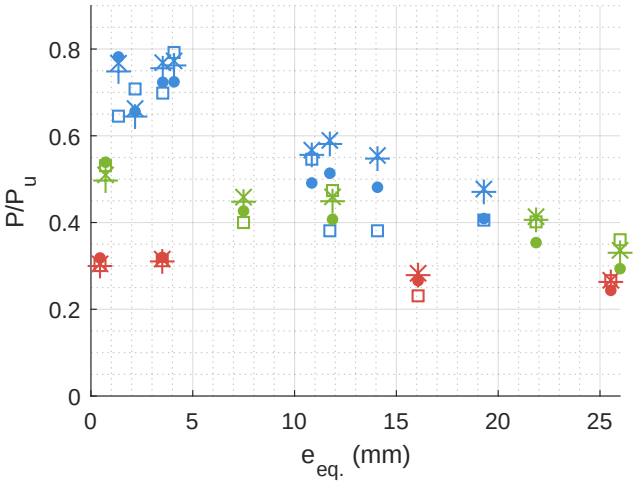


*Figure 9. Comparison between predicted strength with models using measured **EI** and $e_{eq.}$ for each panel, and experimental values.*

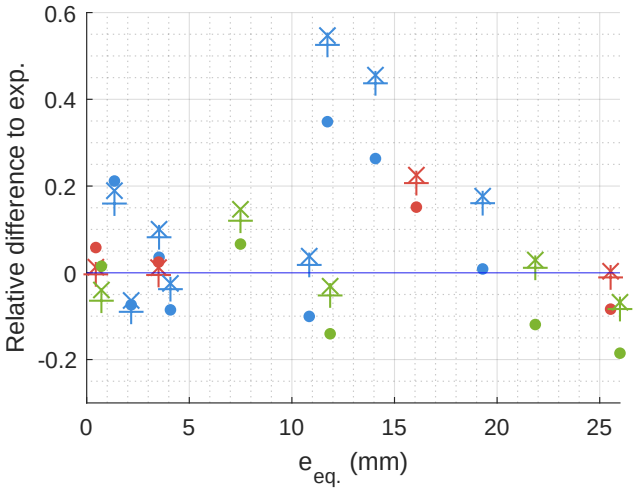


*Figure 10. Relative difference from predicted forces to experimental results, using measured **EI** and $e_{eq.}$.*

can first note that generally, strengths predicted with NLC and measured parameters for each panel are closer to experimental values (see Figure 10). Panels 162 and 172 appear as outliers. We can also note that the influence of load eccentricity on the predicted failure load is smaller for the most slender panels. Whereas for shorter panels, the difference between experimental and predicted values is larger.

## 4.3 Deviation between experimental and predicted values

In order to better compare the error made with the three models, we can calculate the relative deviation from predicted maximal force to experimental maximal force:

$$\text{Relative deviation} = \frac{P_{\max}^{\text{model}} - P_{\max}^{\text{expe.}}}{P_{\max}^{\text{expe.}}} \tag{15}$$

Two sets of relative deviations are calculated corresponding to the two investigated cases

and presented in Figure 11.

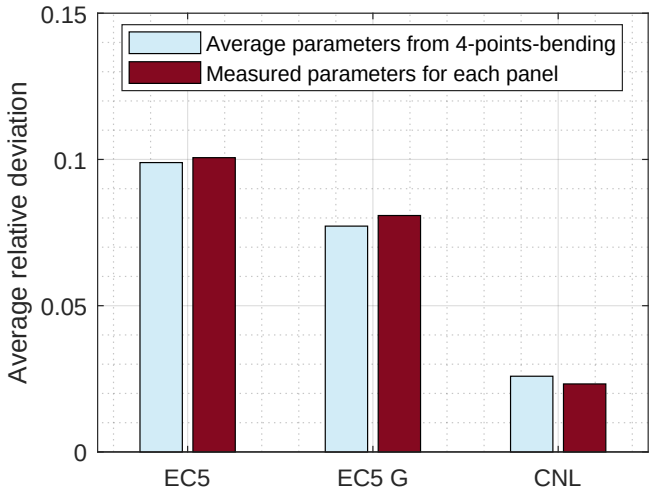


*Figure 11. Average relative deviation from experimental values for Eurocode 5 with or without shear (EC5 G, EC5), and Non-Linear Criterion (NLC).*

We first note that the average relative deviation from experimental values is rather small (around 10% or lower) for all models, and is consistent with material and structural characteristics variability, which are reduced thanks to their precise determination. They are 17% for ***EI*** from buckling tests, 9% for ***EI*** from four-point bending tests, 10% for $E_L$, and 8% for $f_c$. These two cases of calculation could be compared to predicted strengths with normative values from Pfeifer GmbH, 2021. As the mean elastic modulus $E_L$ is underestimated by Pfeifer GmbH, 2021 (11 GPa against 14 GPa measured), we can assume that the difference between predicted strengths with normative values and experimental results would be significantly larger.

We also note that the average relative deviation is lowered for EC5 when shear is taken into account. The Non-Linear Criterion has the lowest average relative deviation (between 2 and 3%, against between 7 and 10% for EC5).

Finally, we can note that there is a small difference between the two cases.

# 5 Conclusion

Buckling tests were conducted on CLT panels that have been precisely characterized, enabling an accurate comparison with Eurocode 5 buckling criterion and a second-order strength criterion considering amplification of all moments the column is subjected to. Thanks to strain and deflection measurements during buckling tests, bending and axial stiffness were measured. An equivalent imperfection taking into account load eccentricity, load location uncertainty, and deviation of the neutral axis from the symmetrical axis caused by material heterogeneity was also determined.

First of all, the standard deviation of the equivalent imperfection is rather large in comparison to Eurocode 5 which assumes an imperfection of L/1000, especially if we acknowledge the fact that imperfection variability is inherent to CLT as it also derives

from material heterogeneity. This measurement is relatively easy to make and enables to properly define boundary conditions of studied panels. Also, interaction diagrams assuming this equivalent imperfection or assuming theoretical eccentricity were presented. It seems that assuming the equivalent imperfection better estimates the moment at failure.

All these parameters also enabled the comparison of predicted force from models and experimental results with the proper determination of different parameters, especially the relative slenderness. The relative deviation from experimental values for each model showed that taking shear into account in Eurocode 5 lowers the deviation, and that the Non-Linear Criterion has the lowest relative deviation.

Nevertheless, with the present data, predicting the maximal force using model with average parameters or panel's specific parameters gives rather similar results. Note that, this conclusion should be taken with caution, as two panels appear as outliers. New experimental campaigns with a larger number of samples may provide a better insight.

# 6 References


Blaß, H. J. & J. Ehlbeck (1987). "Imperfektionsannahmen Für Holzdruckstäbe." In: ISSN: Holz als Roh- und Werkstoff 45 (1987) 231-235.

Christovasilis, I. P.; M. Brunetti; M. Follesa; M. Nocetti & D. Vassallo (Sept. 2016). "Evaluation of the Mechanical Properties of Cross Laminated Timber with Elementary Beam Theories." In: *Construction and Building Materials* 122, pp. 202–213. ISSN: 0950-0618. DOI: 10.1016/j.conbuildmat.2016.06.082. (Visited on 09/01/2021).

EN 1995 1-1 (2005). *Eurocode 5 Conception et Calcul Des Structures En Bois Partie 1-1 : Généralités - Règles Communes et Règles Pour Les Bâtiments*.

GmbH, S. P. T. (2021). *DTU PFEIFER CLT 3.3/21-1043_V1*.

Huang, Z.; D. Huang; Y.-H. Chui; Y. Shen; H. Daneshvar; B. Sheng & Z. Chen (Jan. 2022). "Modeling of Cross-Laminated Timber (CLT) Panels Loaded with Combined out-of-Plane Bending and Compression." In: *Engineering Structures* 250, p. 113335. ISSN: 0141-0296. DOI: 10.1016/j.engstruct.2021.113335. (Visited on 11/02/2021).

Karacabeyli, E. & S. Gagnon (Feb. 2020). *Canadian CLT Handbook, 2019 Edition. Volume I*. Ed. by FPInnovations. Place of publication not identified: National Library of Canada. ISBN: 978-0-86488-590-6.

Kudo, Y.; S. Nakajima; A. Miyatake; Y. Araki; T. Shibusawa & T. Haramiishi (2018). "EVALUATION OF BUCKLING STRENGTH OF CROSS LAMINATED TIMBER STRUCTURAL GRADES." In: *AIJ Journal of Technology and Design* 24.56, pp. 135–140. DOI: 10.3130/aijt.24.135.

Lindner, J.; U. Kuhlmann & A. Just (2016). "Verification of Flexural Buckling According to Eurocode 3 Part 1-1 Using Bow Imperfections." In: *Steel Construction* 9.4, pp. 349–362. ISSN: 1867-0539. DOI: 10.1002/stco.201600004. (Visited on 06/30/2022).

Maitre, P. (Nov. 2013). *Formulaire de la construction métallique selon l'Eurocode 3*. 4e édition. Paris: Le Moniteur. ISBN: 978-2-281-11545-1.

Perret, O.; C. Douthe; A. Lebée & K. Sab (2020). "A Shear Strength Criterion for the Buckling Analysis of CLT Walls." In: *Engineering Structures* 211, p. 110344. ISSN: 01410296. DOI: 10.1016/j.engstruct.2020.110344. (Visited on 07/01/2020).

Perret, O.; A. Lebée; C. Douthe & K. Sab (Oct. 2018). "Experimental Determination of the Equivalent-Layer Shear Stiffness of CLT through Four-Point Bending of Sandwich Beams." In: *Construction and Building Materials* 186, pp. 1132–1143. ISSN: 0950-0618. DOI: 10.1016/j.conbuildmat.2018.07.102. (Visited on 12/16/2020).

Pina, J. C.; E. I. Saavedra Flores & K. Saavedra (Feb. 2019). "Numerical Study on the Elastic Buckling of Cross-Laminated Timber Walls Subject to Compression." In: *Construction and Building Materials* 199, pp. 82–91. ISSN: 09500618. DOI: 10.1016/j.conbuildmat.2018.12.013. (Visited on 04/06/2020).

Shen, Y.; Z. Huang; H. Daneshvar; Y. H. Chui & D. Huang (2022). "Experimental Study of CLT Panels under Combined Out-of-Plane Bending and Compression | Elsevier Enhanced Reader." In: DOI: 10.1016/j.engstruct.2022.115262. (Visited on 11/22/2022).

Theiler, M.; A. Frangi & R. Steiger (Aug. 2012). "Design of Timber Columns Based on 2nd Order Structural Analysis." In.

Thiel, A. & H. Krenn (Aug. 2016). "Buckling Loads for Cross-Laminated Timber Elements under Uniaxial in-Plane Compression." In: *Proceedings of the World Conference on Timber Engineering (WCTE 2016)*. (Visited on 09/30/2020).

van Delft, V. (2020). "Global Buckling Mechanism of Sheet Piles: The Influence of Soil to the Global Buckling Behaviour of Sheet Piles." In: (visited on 06/30/2022).

Wang, J.; M. Mohammad; B. Di Lenardo & M. Sultan (2016). "CLT Panels Subjected to Combined Out-of-Plane Bending and Compressive Axial Loads." In: *World Conference of Timber Engineeing 2016*.